10th International Conference on Short and Medium Span Bridges
Quebec City, Quebec, Canada,
July 31 – August 3, 2018

STRENGTHENING SLENDER STEEL BRIDGE COLUMNS USING A HYBRID FRP SHELL SYSTEM

MacEachern, Daina[1], and Sadeghian, Pedram[2,3]
[1] Department of Civil and Resource Engineering, Dalhousie University, Canada.
[2] Department of Civil and Resource Engineering, Dalhousie University, Canada.
[3] Pedram.Sadeghian@dal.ca

Abstract: In this research, the structural properties of slender steel members reinforced against buckling by fibre-reinforced polymer (FRP) composite shells filled with self-consolidating grout is investigated. In this paper, small-scale models of the proposed system of various diameter of FRP shells were prepared and tested under pure axial loading to determine strength properties. A total of 3 FRP shells were prepared at three inner diameters, namely, 36 mm, 49 mm, and 61 mm, and are 600 mm in length. Cold rolled steel bars, 25.4 mm by 6.35 mm, with lengths corresponding to the FRP shell length were prepared with 44.4 mm long tapered tabs. The self-consolidating grout for filling the shells had a compressive strength of 35.2 MPa and slump flow of 600 mm. Results showed that all systems allowed the steel to reach its yielding load, therefore increasing the overall strength of the member by changing the failure more from buckling to yielding.

1 INTRODUCTION

With the need for rehabilitation or repurposing of existing infrastructure increasing as age and conditions continue to deteriorate, solutions that involve minimal intrusion and planning are in demand (CSCE 2016, ASCE 2016). Economical and efficient solutions that can be applied to improve the condition of slender members, columns, piles and bracings in the field are ideal. Current methods of rehabilitating members include various methods of applying FRP as well as complete removal and replacement of the member with a shop fabricated brace that will allow for higher loading (Black et al. 2004, Tremblay et al. 2006, Harries et al. 2009, Shaat and Fam 2006). These braces are typically steel members encased in a concrete filled steel or FRP tube and are mainly applicable in new construction applications or where the member allows for removal and replacement in field. This paper investigates a new method that would allow for strengthening of the member in field, without removal of the existing member. The system consists of coating the member in a lubricant, wrapping and forming an FRP shell around the member and in-filling with a self-consolidating grout. The technique described in this paper is covered in the recently issued U.S. Patent No. 9,719,255 (Ehsani 2017). This system will allow for free movement of the existing member, allowing it to reach its yield strength, while restraining against buckling. The system will primarily restrict global buckling, however any local buckling within the system will be controlled thought the lateral support of the grout. The objective of this research is to determine the behaviour and structural capabilities of the proposed FRP strengthening system as well as its feasibility to real-life applications. The solution can be applied in the field allowing for the existing member to remain while increasing its buckling capacity. Testing small scale models of the proposed system has allowed for a better knowledge

and understanding of how the system will work and its properties. No set scale was used for the tests, they were used to understand the behaviour and feasibility of the system.

2 EXPERIMENTAL PROGRAM

2.1 Test Matrix

Three specimens were fabricated at a constant FRP shell lengths of 600 mm and three different diameters (36 mm, 49 mm, and 61 mm). Hot rolled steel bars, with 25.4 mm by 6.35 mm cross sections, were prepared to be 35 mm longer than the shell length and 45 mm long tapered tabs were welded on all ends. Steel cores were grouted inside the FRP shell. Specimens are referred to in order of increasing diameter as D1, D2 and D3. More details are provided in Table 1.

Table 1: Test Matrix Details

Specimen ID	Shell Inner Diameter (mm)	Shell Outer Diameter (mm)
D1	36	40
D2	49	53
D3	61	65

2.2 Material Properties

The FRP shells consist of 2 layers of a pre-impregnated FRP laminate made of a biaxial glass fibre fabric, with an over lap of approximately one quarter of the shell circumference, secured with a structural epoxy (adhesive) applied between the layers. Tensile testing was conducted on the FRP laminate as per ASTM ASTM D3039 (2014) and ASTM D7565 (2010). In the warp direction, the test results showed an average modulus of elasticity of 17.16 ± 0.47 GPa, average rupture stress of 192.79 ± 1.54 MPa, average rupture strain of 0.01330 ± 0.00037 mm/mm and a secant modulus of 14,504 ± 285.15 MPa. In the fill direction, the test results showed an average modulus of elasticity of 14.14 ± 0.20 GPa, average rupture stress of 141.16 ± 16.06 MPa, average rupture strain of 0.01162 ± 0.00167 mm/mm and a secant modulus of 12,191 ± 392.6 MPa. Figure 1 contains photos from tensile testing of FRP laminate coupons. The hot rolled steel bars had a tensile yield strength of 310 MPa. The self consolidating grout had a test-day strength of 35.2 MPa (35 days after casting).

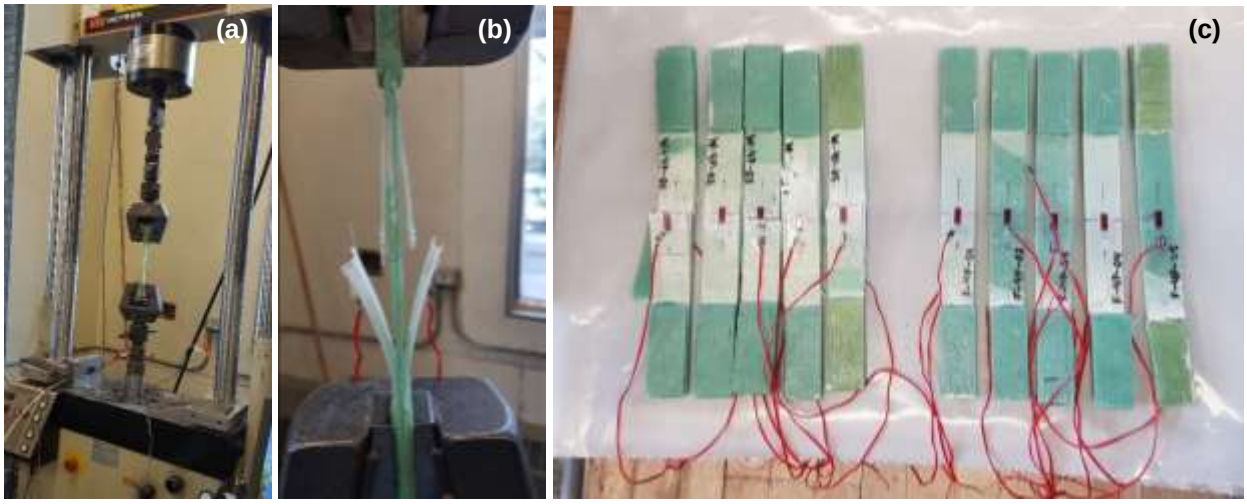

Figure 1: Tensile coupon testing: (a) Test setup; (b) broken coupon; and (c) all tested coupons in the warp and fill direction

2.3 Specimen Fabrication

2.3.1 Shell Fabrication

Sheets of FRP laminate were cut to the appropriate length and width to allow for two wrapped layers with approximately one quarter the circumference in over lap. The material was cut so that the warp direction of the fabric corresponded to the hoop direction of the shell. A two-part structural adhesive was mixed and applied at a uniform thickness of approximately 1 mm over all but one circumference of the shell. Polyvinyl chloride (PVC) pipes were wrapped in a thin layer of plastic to allow for easy removal after curing. The FRP was then slowly wrapped around the tube and secured with another sheet of plastic and taped to secure during curing. Shells were cured for 24 hours and removed from the PVC. Stages of shell fabrication are shown in Figure 2.

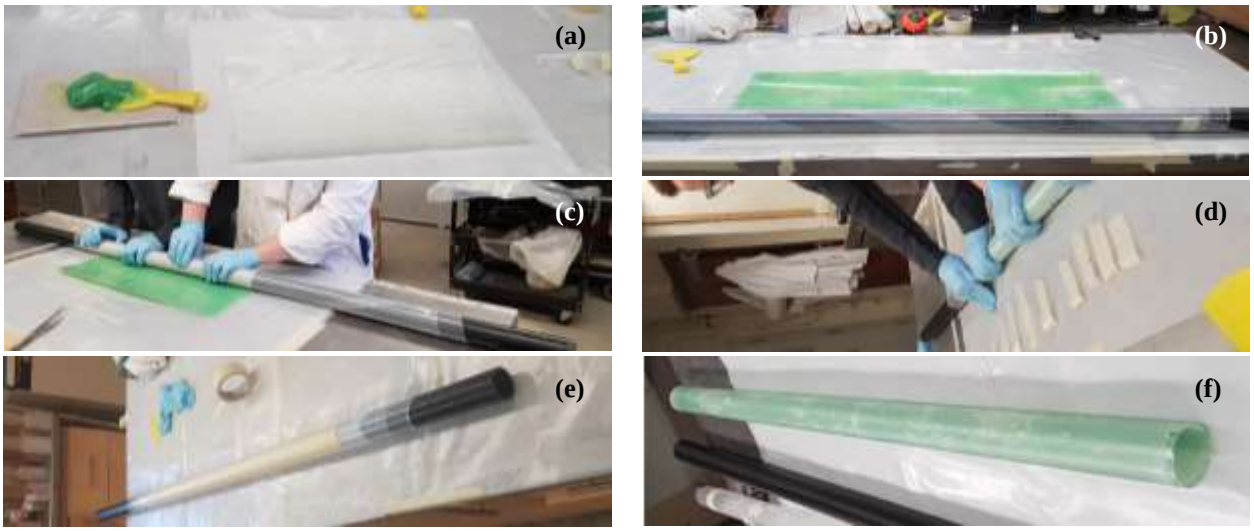

Figure 2: Shell fabrication: (a) FRP Laminate is cut to size; (b) adhesive is mixed and applied to FRP; (c) FRP and adhesive are rolled around PVC tube; (d) FRP shell is secured with plastic sheeting; (e) Plastic sheeting is taped closed and the rolled tube is left to cure for 24 hours; and (f) tube is removed from PVC

2.3.2 Steel Core Preparation

Steel was cut to a length of 635 mm. 45 mm long tabs were cut with 20 mm tapered on one end. These were then welded onto the ends of the steel. 6.35 mm was left on either end to allow for the connection with the test setup. Expanded polystyrene was cut into 25.4 x 6.35 x 25.4 mm pieces and glued on these tabs to limit the transfer of force into the grout under compression. The steel cores were then coated in a thin layer of petroleum jelly to inhibit bonding and interaction between the grout and the steel. Details of the steel core are shown in Figure 3.

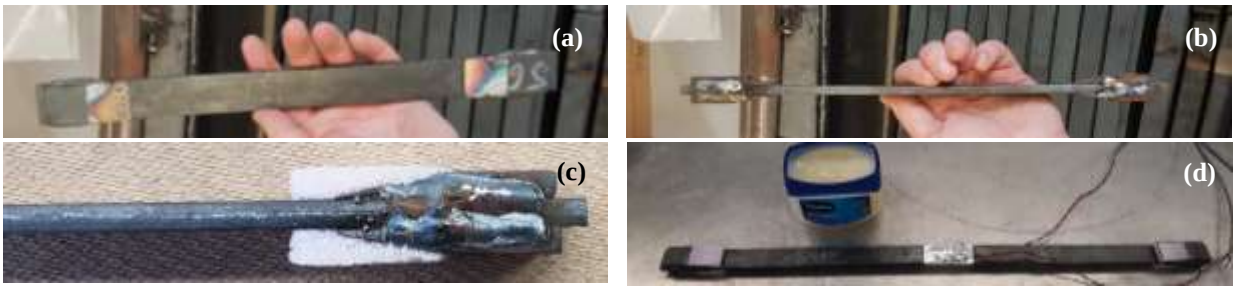

Figure 3: Steel core preparation: (a) Steel core face view; (b) Steel core side view; (c) foam glued to core (side view); and (d) steel core coated in petroleum jelly

2.3.3 Casting and Curing

A stand was fabricated to allow for the specimens to be cast while ensuring the steel core remained vertical and centered in the tube. The FRP shells and steel cores were placed and secured in the frame and the grout was poured between the steel and the shell using a funnel. The slump of the grout was tested using the test method for the slump flow of self-consolidating concrete, ASTM C1611 (2009). Specimens were cured for 28 days before testing. The exposed grout was kept covered by a wet cloth during curing. This process is shown in Figure 4.

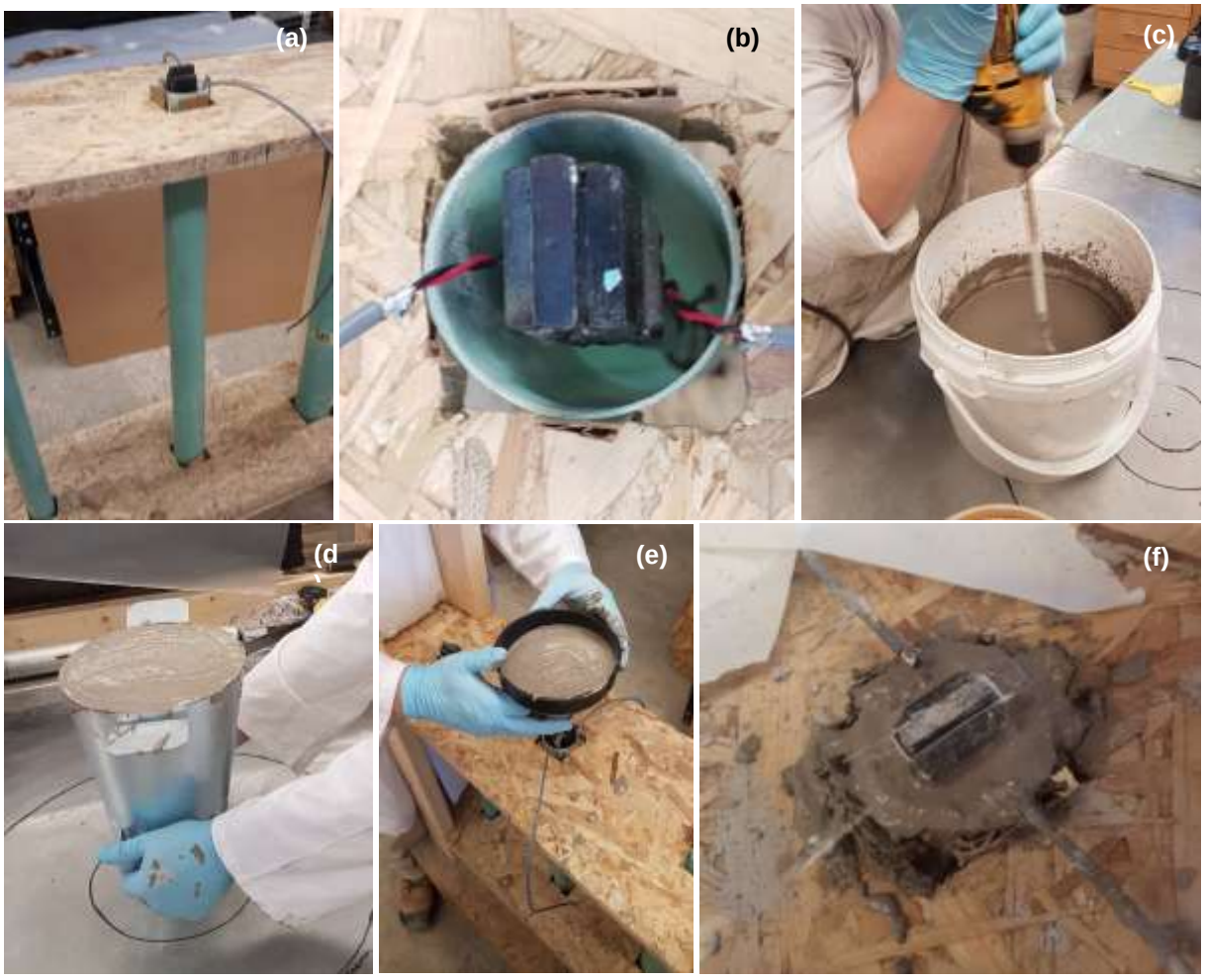

Figure 4: Specimen fabrication: (a) Steel core and FRP tubes are placed in casting stand; (b) tubes are shimmed to ensure steel is centered; (c) grout is mixed; (d) slump test is performed; (e) grout is funnelled into shells; and (f) top plastic cover is positioned to hold steel upright during curing

2.4 Instrumentation and Test Setup

Both ends of each specimen were wrapped with a 75 mm width of basalt fiber using an epoxy resin as the matrix. Two layers were applied with the fibres in the axial direction and two and a half layers were applied with fibres in the hoop direction. This ensured the test results would not be governed by the imperfect end conditions of the test fixture. The test set up simulated pin-pin end conditions.

Two longitudinal strain gauges (SG) were applied at mid-height to each steel core before being cast. Four strain gauges were applied at mid-height to the FRP shell, two in the longitudinal direction and two at 90

degrees to the longitudinal gauges in the hoop direction. The longitudinal strain gauges were applied along the same side as the steel core longitudinal gauges.

Two string potentiometers (SP) were installed along the longitudinal axis of the specimen to measure longitudinal displacement. Two string potentiometers were also installed along the weak axis of the specimen at mid height to measure the lateral displacement due to buckling. The lateral displacement potentiometers failed to record useful data during the three tests and therefore their results were omitted. The test setup is shown in Figure 5.

Final specimens were tested under compression using a universal testing machine with a constant strain loading rate of 2 mm/min. Load, displacement and strain data were collected by a data acquisition system with 10 Hz frequency.

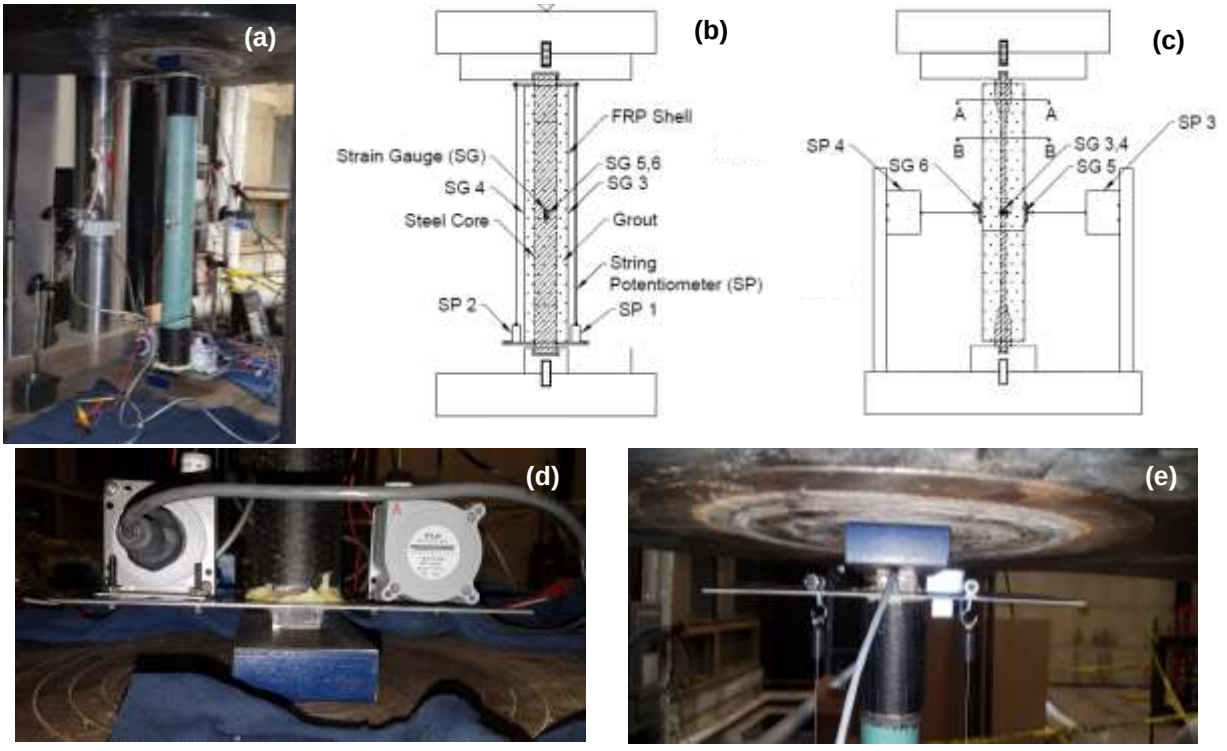

Figure 5: Instrumentation and test setup: (a) Specimen D3 in test setup; (b) test set up face view; (c) test set up side view; (d) base connection and vertical string potentiometer set up; and (e) top connection and vertical string potentiometer hooks

3 RESULTS AND DISCUSSIONS

3.1 Failure Modes

All specimens ultimately failed by buckling at midspan, as seen in Figure 6. Prior to buckling specimens D2 and D3 were determined to have internally yielded, while D1 yielded shortly after or during buckling. While testing specimen D2 it was seen that it compressed to the point at which the concrete may have been loaded. It was recognized with specimen D2 that not enough space was given between the fixture and the shell. For tests D1 and D3, the fixture was cut back to allow more space for the steel to compress. On future tests additional steel will be provided at either end of the shells to ensure there is space for this to happen. Around a load of 110 kN specimen D3 had compressed enough that the plates holding the string potentiometers made contact with the test setup, this allowed for load to be applied to the concrete and shell.

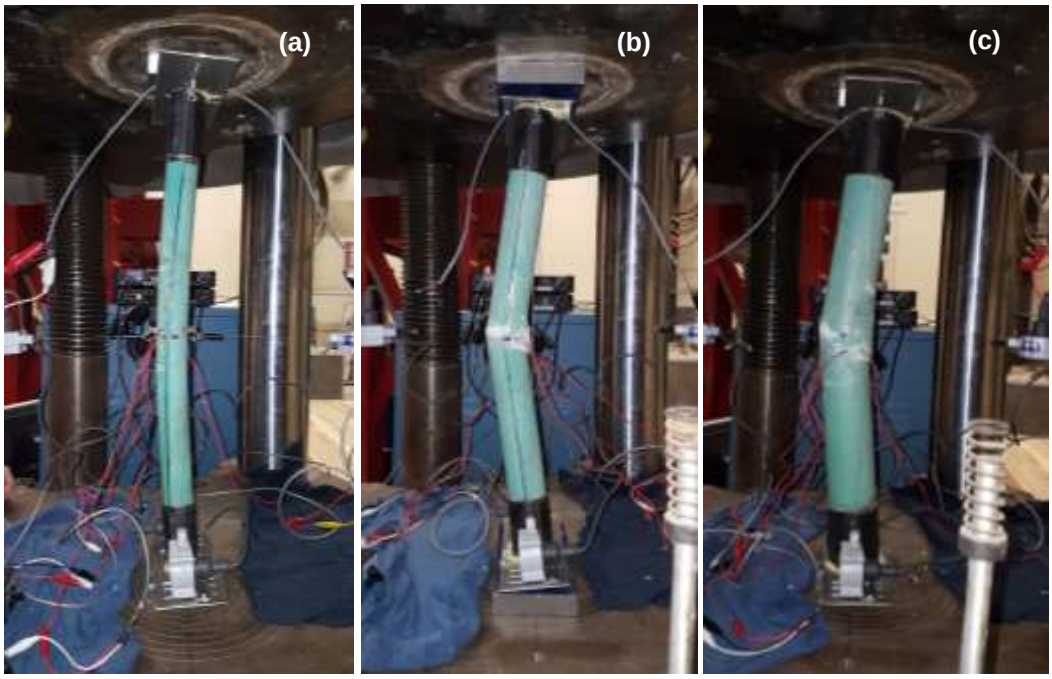

Figure 6: Failure modes of the specimens: (a) D1; (b) D2; and (c) D3

3.2 Load-Displacement Behaviour

Results from the compression tests are given in Table 2 and Table 3. The steel core alone would buckle at a load of 2.65 kN and theoretically yield at a load of 50 kN. For all diameter FRP shell and grout systems the steel was able to reach its yielding load before the system buckled. Figure 7 shows the load vs axial displacement recorded during the three tests. It is seen that the steel yielded between 60-65 kN and buckled at various loads depending on the shell size. All three specimens were tested until buckling occurred. It was found that D2 and D3 were able to reach the yielding failure load of the steel core and then continued to hold load until buckling occurred. Specimen D3 reached a point around 80 kN where the steel core and grout/shell may have begun to act compositely.

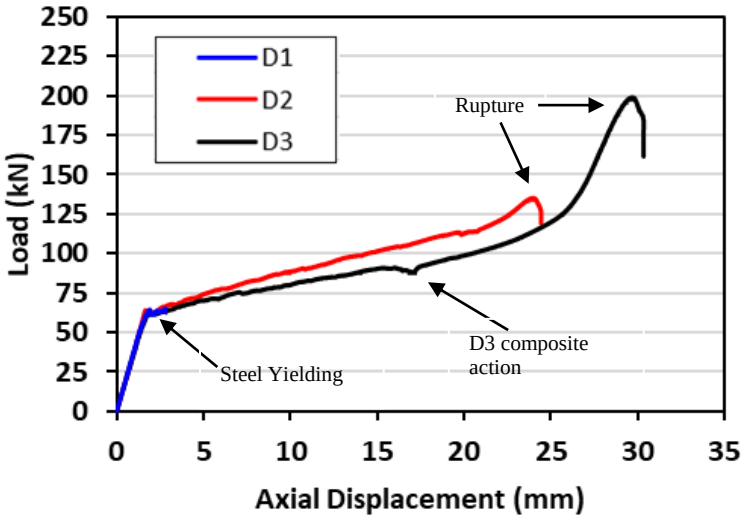

Figure 7: Load vs axial displacement (stroke) of the specimens

Table 2: Test results at yielding

Specimen ID	Yield Load (kN)	Axial Strain in Shell (με)		Shell Hoop Strain (με)
		Compression Side	Tension Side	
D1	64.58	-732	34	90
D2	64.14	-52	-256	44.5
D3	61.95	-70	-92	17.5

Instrumentation errors occurred in the early stages of the tests with the strain gauges applied on the tension side of the steel cores. This is thought to have been caused by tear off once contact was made between the steel cores and the grout. In future tests attempts will be made to limit this issue. Once yielding occurred in all specimens the strain gauge on the compression side of the steel cores also went offline and therefore no data was able to be collected at the ultimate failure state of the system.

Table 3: Test results at peak load

Specimen ID	Peak Load (kN)	Axial Strain in Shell (με)		Shell Hoop Strain (με)
		Compression Side	Tension Side	
D1	65.32	-1304	531	113
D2	135.25	-10227	525	4069
D3	198.89	-8130	-1807	4235

3.3 Load-Strain Behaviour

Strain was recorded on both the FRP shell and the steel core, however, due to premature failure of the strain gauges on the steel as described in section 3.2, the data was not useable. The average hoop strain and both compressive and tensile axial strains recorded on the FRP shell are provided in Figure 8. The separation in the axial strains represents where the specimens began to buckle as one side of the FRP tube began to experience tension while the other side continued to experience an increase in tensile strain.

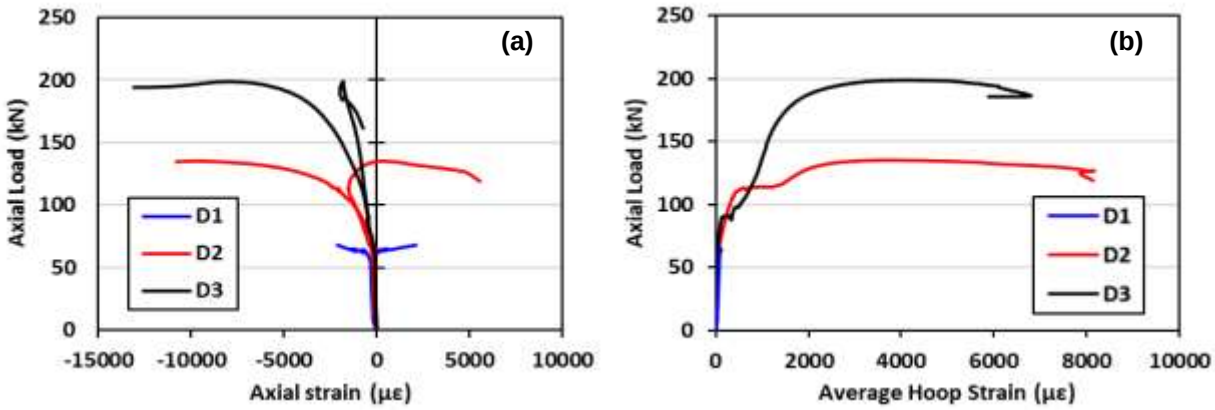

Figure 8: Load vs strain behaviors: (a) load vs axial strain in FRP shell; and (b) load vs average hoop strain in FRP shell

In comparing the hoop and axial strain in Figure 8, as specimens D2 and D3 began to buckle, strain was induced in the hoop direction. In specimen D1 minimal strain was recorded as buckling occurred, this was since the FRP shell did not rupture or expand in the same way as with specimens D2 and D3, as seen in Figure 6. When unloaded, specimen D1 appeared to rebound back to its original shape with little to no damage to the FRP shell. When comparing the axial load vs stroke to the axial load vs axial strain for specimen D1 it appears the steel yielded post-buckling, or around the same time. Specimens D2 and D3 yielded first, followed by both buckling around 100 kN.

4 CONCLUSION

The results from the compression testing of the three specimens show that the proposed system achieved the desired results. All three different diameter specimens achieved their yielding load at or before buckling, representing an increase in strength of around 20 times the plain steel critical buckling load. The results show that the ideal diameter for the core, to achieve these results, is very close to the diameter of specimen D1. The results will be used later to establish a platform to develop reliable design procedures applicable for aging bridges structures. This research will be furthered to include: (i) additional different length specimens to confirm conclusion; (ii) various steel core cross sections; and (i) full scale models. Future small-scale models will be more representative of more common column shapes and configurations. The ratio of the shell diameter to the steel member dimensions will be further studied by a analytical study to predict the optimal shell diameter. The instrumentation issues that occurred during these three tests will be corrected prior to continuing to allow for more accurate and reliable data.

ACKNOWLEDGEMENTS

The authors acknowledge the financial support of Dalhousie University, the Nova Scotia Graduate Scholarship (NSGS), and the National Sciences and Engineering Research Council of Canada (NSERC). The authors also acknowledge QuakeWrap Inc. (Tucson, AZ, USA) for providing GFRP laminate and adhesive. The technical lab support by Jesse Keane and Brian Kennedy of Dalhousie University is appreciated.

REFERENCES

ASCE. 2016. “2017 Infrastructure Report Card.” *ASCE News*.

ASTM. 2009. *C1611/C1611M Standard Test Method for Slump Flow of Self-Consolidating Concrete*. *Annual Book of ASTM Standards Volume 04.02*. ASTM International, West Conshohocken, PA, USA.

ASTM. 2010. *D7565/D7565M - Standard Test Method for Determining Tensile Properties of Fiber Reinforced Polymer Matrix Composites Used for Strengthening of Civil Structures*. *Annual Book of ASTM Standards*. ASTM International, West Conshohocken, PA, USA.

ASTM. 2014. *D3039/D3039M: Standard Test Method for Tensile Properties of Polymer Matrix Composite Materials*. *Annual Book of ASTM Standards*. ASTM International, West Conshohocken, PA, USA.

Black, Cameron J., Nicos Makris, and Ian D. Aiken. 2004. “Component Testing, Seismic Evaluation and Characterization of Buckling-Restrained Braces.” *Journal of Structural Engineering* **130** (6):880–94.

CSCE. 2016. “Canadian Infrastructure Report Card: Informing the Future.” canadainfrastructure.ca.

Ehsani, Mohammad Reza. 2017. Buckling Reinforcement for Structural Members. US 9,719,255 B1. United States Patent, issued 2017.

Harries, Kent A., Andrew J. Peck, and Elizabeth J. Abraham. 2009. “Enhancing Stability of Structural Steel Sections Using FRP.” *Thin-Walled Structures* **47** (10): 1092–1101.

Shaat, Amr, and Amir Fam. 2006. “Axial Loading Tests on Short and Long Hollow Structural Steel Columns Retrofitted Using Carbon Fibre Reinforced Polymers.” *Canadian Journal of Civil Engineering* **33** (4):458–70.

Tremblay, R, P Bolduc, R Neville, and R DeVall. 2006. “Seismic Testing and Performance of Buckling-Restrained Bracing Systems.” *Canadian Journal of Civil Engineering* **33** (2):183–98.